# Evolution of Coal Permeability under Combined Thermo-Mechanical Impact Loading

Shiyi Cheng, Fuchao Tian, Jiahao Su

Abstract—To probe the variation rule of coal permeability after crushing under different temperature-impact force compound fields, according to the fractal theory and classical models, the static and dynamic strains of coal are analyzed, and a coal permeability model under the composite field is derived. Through the impact crushing influent experiments under different temperature - impact force, the following conclusions are summarized:(1) When p < 1.0p<1.0 MPa, affected by the temperature-impact load, the coal seepage channels become narrower, and the permeability shows an approximately decreasing exponential decline with temperature. When 1.0 MPa ≤p<10.0 MPa, under the action of the impact force, the seepage passageway is wider and their quantity increases. The permeability shows an approximately exponential upward trend with based on the pore impact force. When p≥10.0 MPa, the impact force reaches the ultimate resistance pressure force, the coal is fractured and broken, released the impact energy, and the fissure structure becomes stable, resulting in the permeability tending to be steady.(2) The coal seepage process pass through two processes: the susceptible temperature seepage stage and the susceptible impact force seepage stage.(3) Under a small impact force, the coal permeability decreases, accompanied by the slip effect. After the impact force reaches the ultimate tensile force of the coal, the coal experiences radial and circumferential rupture, the slip effect weakens, and the permeability increases.

Index Terms—temperature-impact force; impact-crushing; static-dynamic permeability; sensitivity threshold; slippage effect

#### I. INTRODUCTION

t present, the study of coal and rock fracturing Amechanisms and low-permeability coal and rock has become a topic of great interest among contemporary scholars. Numerous researchers have investigated the of various coal and rock types under different element (such as water, CO<sub>2</sub>, N<sub>2</sub>, and mercury) and extreme conditions [1]-[5]. Q. Qi, X. Fu, B. Qiu et al [6],[7], proposed that the vaporization of liquid nitrogen generates thermal stress and expansion stress, thereby enhancing coal reservoir permeability. Z. Lu et al [8], high-pressure nitrogen analog and methane adsorption-desorption experiment was employed to quantify void characteristics of the coal samples. Z. Wang, H. Li dated the macroscopic damage mechanism of coal fracturing. Y. Li, X. Jiang et al [10], sure an initiation model, revealing that the propagation distance of fracture is inversely related to the viscosity of the fracturing fluid and directly related to

Manuscript received Apr 9, 2025; revised Aug 8, 2025.

This work was received joint funding from the National Natural Science Foundation of China (Grant Nos. 52174230) and the Natural Science Foundation of Liaoning Province (Grant Nos. 2022-KF-23-03).

Shiyi Cheng is a researcher of China Coal Research Institute Fu shun Branch, Shenfu Demonstration Zone 113122 China (e-mail:syixiaoheimai127@126.com). Fuchao Tian is a researcher of China Coal Research Institute Fu shun Branch, Shenfu Demonstration Zone 113122 China (e-mail: tianfuchao@cumt.edu.cn).

Jiahao Su is an engineer of Yulin Yushen Coal Yushuwan Coal Mine Co., Ltd., Yulin, 719000, China (e-mail: <a href="mailto:15670880885@163.com">15670880885@163.com</a>).

the viscosity of the fracturing fluid and directly related to the fracture width, additionally, the time function of the CH<sub>4</sub> displacement radius was analyzed  $y=Ae^{\beta t}+y_0$  X. Chang, E. Xu et al[11], pointed out that the process of coal seam fracturing consists of five stages: stress accumulation, fracture initiation, fracture propagation, multiple fracture initiation propagation, and final fracture extension.

Prior investigations into coal and rock fracture have largely been confined to studies of homogeneous materials, isolated variables, sequentially applied multipara-meter conditions, or observational analyses restricted to either the micro-scale[12]-[15]. However, research on fracturing under the influence of composite dynamic media remains scarce. Additionally, the relationship between onsite coal seam fracturing effectiveness and influence factors such as fracturing pressure is not yet clearly defined. Therefore, this paper draws on prior research regarding the effects of temperature and pressure on coal permeability to propose a multi-stage permeability model for nitrogen fracturing of coal under a combined temperature impact loading field. Using nitrogen under vary temperature and impact loading as the comprehensive fracturing load, impact-fracture seepage experiments was conducted under different temperature and impact loading conditions. The rationality of the derived model was analyzed, and the permeability patterns of coal fractured by nitrogen under different temperature and impact loading conditions were summarized.

#### II. MULTI-STAGE PERMEABILITY MODEL

A. Multi-Stage Permeability Model of Nitrogen Fracturing in Coal under Combined Field Conditions

Based on the classical S&D model, crack propagate on models[16],[17], and fractal seepage models[18],[19] ,the permeability of coal under the combined effects of temperature and impact loading can be divided into two stages: static permeability and dynamic permeability: static permeability occur when the gas-induced pore impact force is below the critical resistance value of the coal. During this stage, the coal matrix undergoes static volumetric strain (including adsorption deformation, expansion deformation, and thermal cracking deformation) due to the combined effects of temperature and impact loading; dynamic permeability occurs when the gas-induced pore impact force exceeds the critical resistance value of the coal. Here, the coal fracture under dynamic strain (such as fracture dilation deformation) under the combined effects of temperature and impact loading.

- a. Analysis of Static Strain
- (1)Temperature and impact-dependent nitrogen adsorption deformation in coal quantified by the Langmuir isothermal adsorption model[20]. The formula for adsorption deformation under varying temperatures is introduced as follows:

$$\varepsilon_f = \frac{3\rho_c a R_c T}{V_0 E_A} ln \frac{1 + bp}{1 + bp_0} \tag{1}$$

In the formula:  $\mathcal{E}_f$  is volume strain induced by coal adsorption;  $\rho_c$  is coal density,  $g/cm^3$ ;  $p_0$  is initial gas pressure, MPa; p is gas pressure, MPa;  $E_A$  is swelling modulus induced by adsorption, MPa; T is initial Temperature, C;  $V_0$  is standard molar volume, 22.4L/mol;  $R_c$  is gas constant,  $8.314\ J/kmol$ ;  $R_c$  b is gas adsorption constant.

(2) Characteristics of Coal Swelling Deformation: Under the influence of a high-temperature field, the internal structure of the coal matrix undergoes expansion and deformation due to temperature effects. Assuming the coal structure undergoes isotropic deformation, the thermal expansion strain of coal[21] is expressed as:

$$\varepsilon_c = a_T \Delta T \tag{2}$$

In the formula:  $\varepsilon_c$  is volume strain induced by thermal expansion;  $a_T$  is thermal expansion coefficient;  $\Delta T$  is temperature increment;

(3) Characteristics of Coal Thermal Cracking Deformation: When the moisture in coal evaporates due to high temperatures, leading to the development of new pores or microfractures in the coal matrix structure, the formation of these pores and fractures caused by heating is referred to as the thermal cracking deformation of coal [22] is expressed as:

$$\varepsilon_{\tau} = \varphi_m - \varphi_0 \tag{3}$$

In the formula:  $\varepsilon_r$  is thermal cracking deformation of coal;  $\varphi_m$  is porosity of coal matrix;  $\varphi_0$  is initial porosity of coal matrix;

#### b. Dynamic Strain Analysis

As posited in previous research, the process of high-pressure gas impact on coal results in a sequence of events. Firstly, an initial stress impact phase is undergone by the fractures in the coal pore walls. This is followed by a static phase [23]. Specifically, in stances where the impact force of the high-pressure gas is less than the ultimate compressive strength but greater than the ultimate tensile strength of the coal, the pores undergo compressive failure, resulting in the formation of radial fractures. The heterogeneity of the coal matrix is a primary factor contributing to the irregular deviation of radial movement, which in turn generates shear forces between coal bodies. This phenomenon ultimately leads to shear failure. As the impact load attenuates, fractured units develop stress directed towards the center, forming circumferential fractures. The combination of these two types of fractures creates a fracture zone, the maximum radius of which can be calculated using the following formula:

$$R_{\text{max}} = \left(P / S_{td}\right)^{\frac{1}{\alpha}} \alpha \tag{4}$$

In the formula: P is gas impact load, MPa;  $S_{ut}$  is ultimate tensile strength of the coal, MPa;  $\alpha$  is attenuation coefficient,  $\alpha = (2-\mu)/(1-\mu)$ ;  $\mu$  is 0.8 times the static Poisson's ratio;

Taking radial and circumferential fractures in the fracture zone as the calculation objects, the radius of the fracture zone is incorporated into the calculation of fracture volume, explain of the central Angle of circular fractures  $\theta$ , derivation of the arc length formula for circumferential fractures:

$$\mathbf{L}_{H} = \iint d\mathbf{R}_{H} d\boldsymbol{\theta} = (\mathbf{R} - \mathbf{R}_{0}) (\boldsymbol{\theta}_{\text{max}} - \boldsymbol{\theta}_{\text{min}}) \qquad (5)$$

In the formula:  $L_H$  is circumferential arc length,  $\mu m$ ;  $R_H$  is circumferential radius,  $\mu m$ ,  $R_H \in [R_0, R_{\max}]$ ;  $\theta$  is central angle of circumferential fractures, rad,  $\theta \in [\theta_{\min}, \theta_{\max}]$ ;

Citing fractal [24],[25] theory the number of cracks in coal under impact loading can be expressed as:

$$-dN = D_f \lambda_{\text{max}}^{D_f} \lambda^{-D_f - 1} d\lambda$$
 (6)

In the formula: N is denotes the number of pores and fractures;  $D_r$  is pore-fracture fractal dimension;  $\lambda \cdot \lambda_{\max}$  is fracture width and maximum fracture width;  $D_0$  is initial fractal dimension;

Under radial and circumferential impact loads, coal forms quasi-cylindrical curved fracture channels. In scenario, the load-bearing areas of radial and circumferential fractures are  $S_J$  and  $S_H$ , expressed as follows:

$$dS_{J} = \lambda \pi (R - R_{0}) dN \tag{7}$$

$$dS_{H} = \lambda \pi L_{H}(-dN) \tag{8}$$

Follows to

$$S_{J} = \int_{\lambda_{\min}}^{\lambda_{\max}} \lambda \pi (R - R_{0})(-dN) = \pi (R - R_{0}) \cdot D_{f} \lambda_{\max} \left[ 1 - \left( \frac{\lambda_{\min}}{\lambda_{\max}} \right)^{(1 - D_{f})} \right]$$

$$(9)$$

$$S_{H} = \int_{\lambda_{\min}}^{\lambda_{\max}} \lambda \pi L_{H} D_{f} \lambda_{\max}^{D_{f}} \lambda^{-D_{f}-1} d\lambda = (R - R_{0}) \bullet$$

$$(\theta_{\max} - \theta_{\min}) \pi D_{f} \lambda_{\max} \left[ 1 - \left( \frac{\lambda_{\min}}{\lambda_{\max}} \right)^{(1 - D_{f})} \right]$$
(10)

In the formula:  $\lambda$  is fracture width,  $\mu$ m,  $\lambda \in [\lambda_{\min}, \lambda_{\max}]$ ;  $R_0$  is coal pore radius, mm;

When the impact load on the coal pore wall is lower than the ultimate compressive strength of the coal, the coal generates circumferential tensile stress exceeding its ultimate tensile strength during compression. This leads to tensile deformation, forming radial fractures. meanwhile, influenced by heterogeneous media and differential displacement of unit bodies, shear stress develops, causing shear failure and the formation of shear fractures.

Effective strain formula for radial fractures as follows:

$$\varepsilon_{J} = \frac{P_{H}}{S_{J}G_{0}} = \frac{1}{G_{0}\pi D_{f}\lambda_{\text{max}}} \cdot \frac{1}{1 - \left(\frac{\lambda_{\text{mix}}}{\lambda_{\text{max}}}\right)^{(1-D_{f})} \cdot \frac{P_{H}}{R - R_{0}}}$$
(11)

Effective strain formula for circumferential fractures as follows:

$$\mathcal{E}_{H} = \frac{P_{J}}{S_{H}G_{0}} = \frac{1}{G_{0}\pi D_{f}\lambda_{\text{max}}} \cdot \frac{1}{1 - \left(\frac{\lambda_{\text{min}}}{\lambda_{\text{max}}}\right)^{(1-D_{f})} \cdot \left(R - R_{0}\right) \left(\theta_{\text{max}} - \theta_{\text{min}}\right)} \tag{12}$$

In the formula:  $P_{H}$  is circumferential load on coal pores, MPa; is radial load on coal pores, MPa;  $G_{0}$  is Young's Modulus of coal fractures, GPa;

During coal borehole fracturing, under the combined effects of temperature field and impact loading field, coal undergoes successive volume changes in four forms: adsorption, swelling, thermal cracking and dilation. Volumetric strain of coal  $\varepsilon_Z$  as follows:

$$\varepsilon_{z} = \varepsilon_{f} + \varepsilon_{c} + \varepsilon_{r} + \varepsilon_{J} + \varepsilon_{H} = \frac{3\rho_{c}aRT}{V_{0}E_{A}} ln \frac{1 + bp}{1 + bp_{0}} + \frac{1}{G_{0}\pi D_{f}\lambda_{\text{max}}} \cdot \frac{1}{1 - \left(\frac{\lambda_{\text{mix}}}{\lambda_{\text{max}}}\right)^{(1-D_{f})} \cdot \frac{1}{R - R_{0}}} \cdot (13)$$

$$\left(P_{H} + \frac{P_{J}}{\theta_{\text{max}} - \theta_{\text{min}}}\right)$$

Based on the Reynolds equation, fractal seepage theory, and Hooke's law, the relationship between coal permeability and volumetric strain under the dual impacts of temperature field and impact stress field is derived. The resulting multi-stage permeability formula for nitrogen fracturing coal under dual effects is obtained.

When the impact load exceeds the ultimate tensile strength of coal, the coal is primarily subjected to combined impact loading and thermal effects. The fractures undergo impact-driven evolution, with the impact load dominating fracture development. According to the permeability-strain

formula derived from the Reynolds equation [26], the permeability of coal can be expressed as:

$$k = k_{0}e^{\left(\varepsilon_{f} + \varepsilon_{c} + \varepsilon_{r} + \varepsilon_{J} + \varepsilon_{H}\right)} = \begin{bmatrix} \frac{3\rho_{c}aRT}{V_{0}E_{A}} ln \frac{1 + bp}{1 + bp_{0}} + a_{T} \triangle T + (\varphi_{m} - \varphi_{0}) + \frac{1}{G_{0}\pi D_{f}\lambda_{\max}} \frac{1}{1 - \left(\frac{\lambda_{m/x}}{\lambda_{\max}}\right)^{(1-D_{f})} \cdot \frac{1}{R - R_{0}} \cdot \end{bmatrix}$$

$$k_{0}e^{\left(\varepsilon_{f} + \varepsilon_{c} + \varepsilon_{r} + \varepsilon_{J} + \varepsilon_{J}\right)}$$

$$(14)$$

When the borehole impact load is less than the ultimate tensile strength of coal, the combined action of impact load and temperature induces radial fractures in coal, accompanied by slip effects. The fractal permeability of coal under the dual-field (impact-temperature) can be expressed as:

$$k = k_{a} \left( 1 + \frac{B}{P} \right) e^{\left(\varepsilon_{f} + \varepsilon_{c} + \varepsilon_{r} + \varepsilon_{f}\right)} = k_{a} \left( 1 + \frac{B}{P} \right) \bullet$$

$$\left[ \frac{\frac{3\rho_{c}aRT}{V_{0}E_{A}} ln \frac{1 + bp}{1 + bp_{0}} + a_{T} \triangle T + (\varphi_{m} - \varphi_{0}) + \frac{P_{H}}{Q_{0}}}{G_{0}(R - R_{0})\pi D_{f} \lambda_{\max}} \left[ 1 - \left( \frac{\lambda_{\min x}}{\lambda_{\max}} \right)^{(1 - D_{f})} \right] \right]$$

$$(15)$$

In the formula:  $k_0 \sim k_a$  initial permeability and absolute permeability (10<sup>-3</sup>  $\mu m^2$ ); B is gas slippage factor;

# III. MULTIPHYSICS PERMEABILITY EXPERIMENTS

A. Temperature and Pressure Nitrogen-Driven Coal B orehole Impact-Fracturing Seepage Experiment

#### a. Experimental Preparation

For this experiment, 50 standard specimens for  $\Phi 50mm \times 100mm$  were prepared from coal samples extracted from a coal seam in a mine. The tests were conducted using a high-temperature and high-pressure nitrogen seepage-fracturing experimental setup, as Fige 1.

#### b. Experimental Scheme

To study the variation law of coal permeability under the impact of high-temperature and high-pressure nitrogen pore fracturing, 99.99% nitrogen was selected as the fracturing medium to conduct the permeability-fracturing test of coal under the dual fields of temperature and impact load. Based on the in-situ stress, the compressive strength of 10.0 MPa and the tensile strength of 1.0 MPa of the coal sample, The test temperature is selected as 20°C, 40°C, 70°C, 100°C, and 200°C, and the impact load was applied at an increment of 0.2 MPa. Fracturing was performed under different impact loads at each temperature, and the seepage rate of coal was measured.

In the experiment, after completing the system air tightness

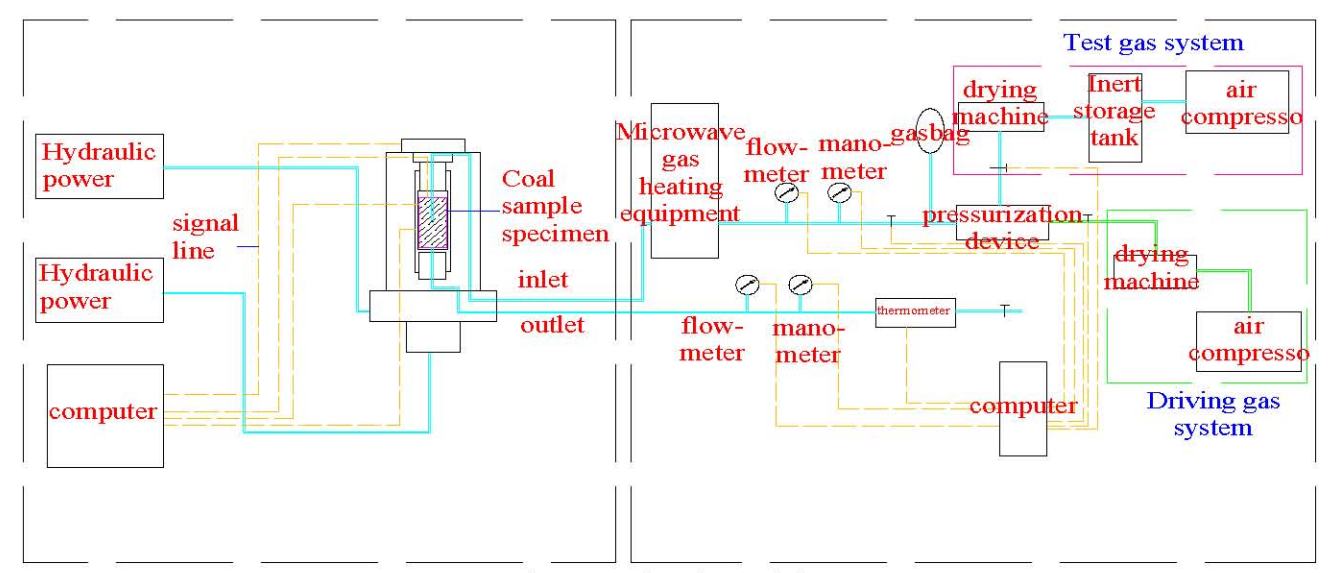


Fig.1 Seepage fracturing test device

test and simulating the confining pressure field, nitrogen is heated to 20°C by a rapid microwave heater and the temperature is controlled. A pressure-boasting and pressure-maintaining pump is used to control the nitrogen impact pressure. Pore impact fracturing is carried out with coal pore impact loads of 0.2 MPa、0.4 MPa、0.8 MPa、1.0 MPa、1.4 MPa、2.2 MPa、3.2 MPa、5.0 MPa、6.8 MPa、8.0 MPa、10.0 MPa and 12.0 MPa. The radial and circumferential loads of the coal pores are measured. The maximum value of the impact load is 15.0 MPa and each load acts for 24t. After the inlet and outlet gas pressures and gas flow rates are stable, the data are recorded, and the permeability of coal under nitrogen pressure with different impact loads at 20°C is calculated. The entire test channel and device are insulated to avoid temperature loss, and the temperature sensors at the inlet and outlet are used to record the changes in the temperature field. The coal sample is replaced, and the above test process is repeated for tests under different impact loads at 40°C, 70°C, 100°C, and 200°C. The permeability under different conditions is calculated according to Darcy's law, and the slip effect of nitrogen in the coal body is judged through the flow rate changes.

c. Analysis of the Critical Permeation Law of Coal under the Action of Nitrogen Fracturing in a Composite Field

High temperature and high impact pressure are the main factors affecting coal fracturing and permeation. To study the law and sensitivity of coal permeability under high temperature and high impact pressure, the following analysis is carried out based on the above test results. Figure 2 shows the relationship curve between coal permeability and impact force at different temperatures; Figure 3 shows the relationship curve between coal permeability and temperature under different impact force when the impact force is less than the ultimate failure force of coal. It can be seen from Fig 2 and Fig 3.

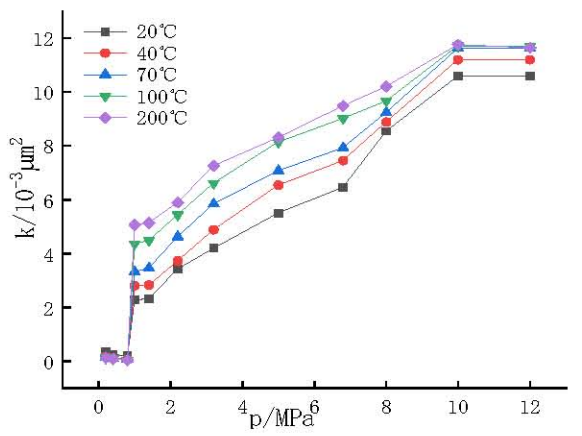


Fig.2 Relationship between coal permeability and impact load under different temperatures

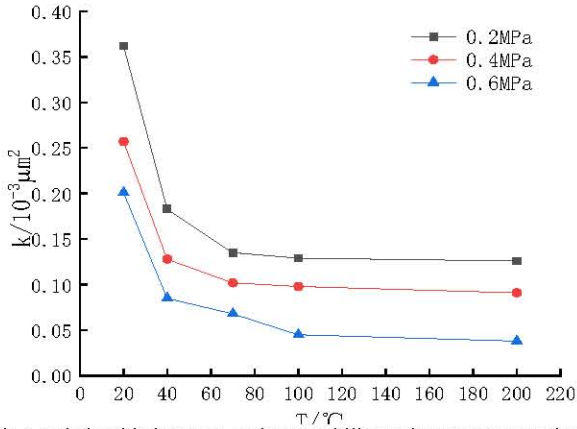


Fig.3 Relationship between coal permeability and temperature under different impact loads

- (1) In the case where the impact load p < 1.0p<1.0 MPa, the adsorptive behavior, thermal cracking phenomena, and expansion related deformation of the coal matrix are in direct proportion to the temperature. Affected by the confining pressure, the volumetric strain of the coal is in inverse proportion to the temperature.
  - (2) When the temperature remains constant, under the

combined action of the temperature-impact pressure dua-field, when the impact load p < 1.0 MPa, the permeability shows an approximately exponential decline trend with based on the pore impact force. During the fracturing process of coal under the temperature impact load, the impact load is much smaller than the ultimate resistance load of the coal. Affected by the temperature and the impact force, the movement of the adsorbed gas molecules inside the raw coal becomes active, the pore and matrix structures change, resulting in expansion and the formation of new pores, and internal structural changes such as adsorption deformation, expansion deformation, and thermal cracking deformation occur. Since the external structure of the coal remains stable, the seepage channels become narrower and less smooth, leading to a decrease in permeability; When the impact load 1.0 MPa $\leq p \leq 10.0$ MPa, the permeability shows an approximately exponential increase trend with the increase of the pore impact load. As the impact force achieve the ultimate resistance tensile force and is less than the ultimate resistance compressive load, the internal structure that tends to be in a static deformation state is affected by the impact force. The original pores and fractures develop both horizontally and vertically, generating new radial or circumferential fractures, which leads to wider seepage channels and an increase in their quantity, thus increasing the permeability; When the impact load  $p \ge 10.0$  MPa, the permeability shows a gentle trend with the increase of the pore impact load. As the impact force achieve the ultimate resistance compressive force, the coal under goes impact fracture, the impact load is released, and the development of coal fractures gradually stabilizes, causing the permeability to tend to be stable.

(3) When the impact load p < 1.0 MPa, the change rate of coal permeability based on the impact load field is relatively gentle, while there are obvious changes based on the temperature field. This indicates that in this process, the coal undergoes adsorption deformation, expansion deformation, and thermal cracking deformation under the action of temperature, and the permeability is more sensitive to the influence of temperature; When the impact load  $p \ge 1.0$  MPa, the coal permeability increases sharply, indicating that when the impact force reaches the ultimate tensile force of the coal, obvious new fissure are generated in the coal structure, and the permeability is more sensitive to the influence of the impact load.

In conclusion, under the combined action of the high - temperature and high - pressure dual - field, the coal pore impact fracturing causes the coal seepage to go through two stages: the temperature - sensitive seepage stage and the impact - pressure - sensitive seepage stage. When the impact force is less than the ultimate tensile force, the coal seepage is more sensitive to the influence of the temperature field, and the coal pore impact fracturing belongs to the static fracturing stage. When the impact load is greater than the ultimate tensile load and less than the ultimate compressive load, the coal seepage is more sensitive to the influence of the impact pressure field, and the coal pore impact fracturing belongs to the dynamic fracturing stage.

TABLE I MIBDEL PARAMETER

Parameter	value	source
$k_{O}$	$0.25 \times 10^{-3}$	self-test
M	28	Molar mass of nitrogen gas molecules
$R_c$	8.314	Gas constant
$V_{\mathcal{O}}$	22.4	Molar volume
$E_A$	1900	self-test
$a_T$	2.4×10 <sup>-5</sup>	self-test
$ ho_c$	1.316	self-test
$G_{0}$	0.029	self-test
$R_0$	5	self-test
$R_{max}$	35	self-test
$D_{\theta}$	1.124	self-test
$\varphi_0$	0.056	self-test
$S_{td}$	1	self-test
$\Theta_{min}$	0.0128	self-test
$\Theta_{max}$	0.0361	self-test

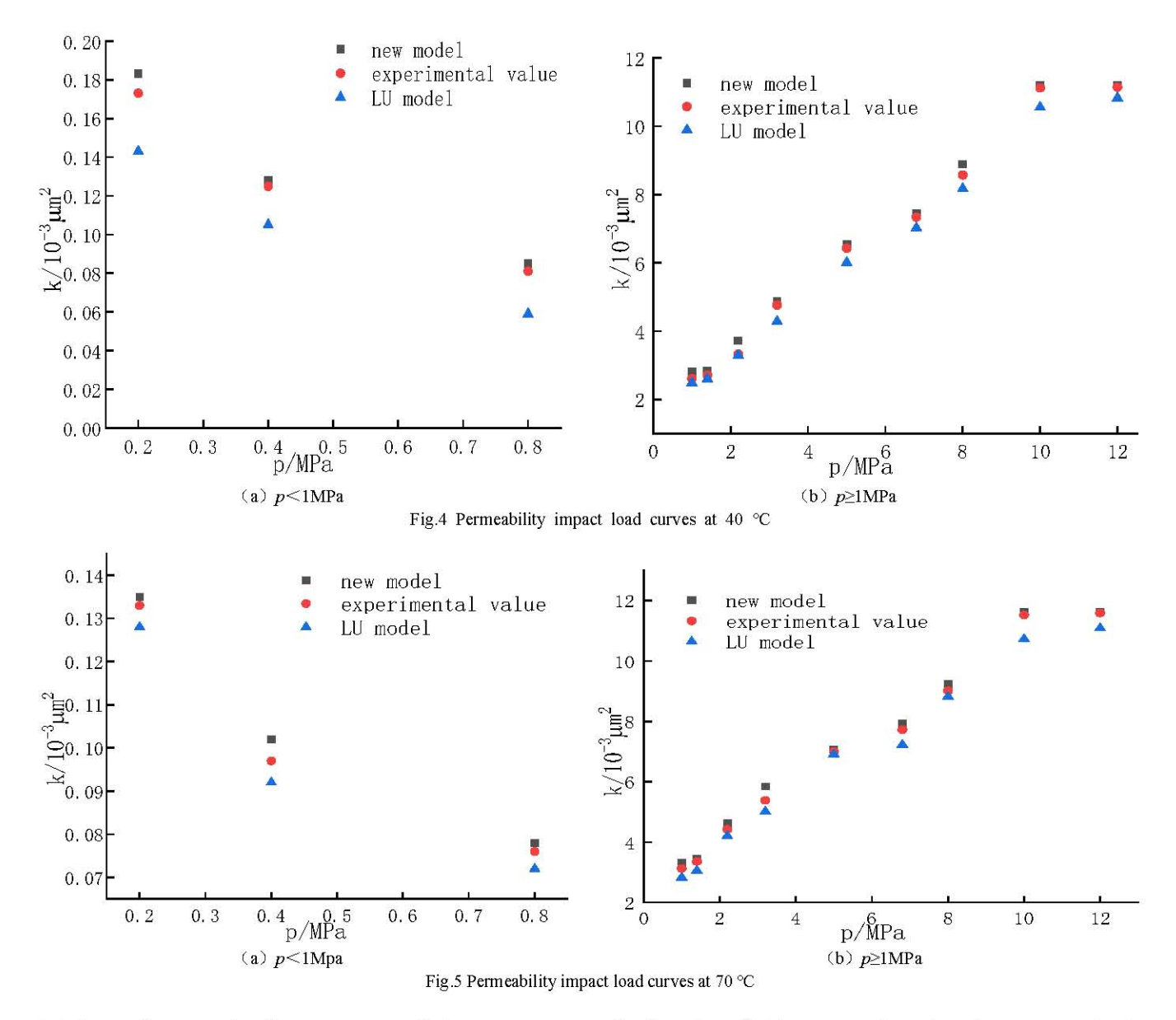
### d. Model Comparative Analysis

To verify the rationality of the coal permeability model under the application of the impact load temperature composite field in coal pores, the model data and test parameters in Table I are substituted into the new model and the LU permeability model. The corresponding permeability is calculated and compared with the test permeability. Fig 4 shows the permeability-impact load curve at a temperature of 40 °C, and Fig5 shows the permeability-impact load curve at a temperature of 70 °C.

As can be seen from the above figures, the calculated values of the new model are in better agreement with the experimental value curves. The values of the new model and the experimental values are greater than those of the LU permeability model. This indicates that under the action of a relatively small impact load, coal at different temperatures undergoes adsorption, expansion, and thermal cracking, resulting in a decrease in permeability. Inert nitrogen slows down the adsorption deformation of coal and alleviates the attenuation of permeability, leading to the occurrence of the slip effect. After the impact force achieve the ultimate tensile load of the coal, the impact load forms a fracturing impact from the inside to the outside of the coal. The original fractures inside the coal expand, and new radial (circumferential) fractures are generated, causing the permeability to increase.

#### IV. CINCLUSION

(1) The impact load of 1.0 MPa is the critical threshold, beyond which the adsorption, thermal cracking and expansion deformation of the coal matrix are directly proportional to the temperature. The confining pressure exerts an effect on the volumetric strain of the coal, the nature of which his such that



it is inversely proportional to temperature. It is at pressures of  $p \ge 1.0$  MPa that the coal body is subject to the ultimate load, with the occurrence of obvious fracture deformation. The strain effect of the matrix is reduced, and the volumetric strain of the coal is directly proportional to the impact load.

(2) Under temperature constant and impact load p < 1.0MPa, coal permeability exhibits an approximate exponential decline trend with increasing impact load. Given that the impact load is significantly lower than the coal's ultimate resistance load, the coupled effects of temperature and impact load induce enhanced mobility of adsorbed gas molecules within the coal matrix. This results is adsorption deformation, expansion deformation and thermal cracking deformation, due to the external structure of the coal less stable, resulting in narrower, less fluid permeable channels and reduced permeability The impact load (1.0 MPa ≤ P < 10.0 MPa) has a significant impact on the internal structure of the coal, affecting it to a greater extent than the ultimate resistance tensile load. The initial pores and fractures manifest both horizontally and vertically, giving rise to new radial or circumferential fractures. These, in turn, result in the formation of wider seepage channels and an augmentation in their number. The permeability demonstrates an approximate exponential increase trend with the escalation of the pore impact force. The impact loads of 10.0 MPa and above, the impact load attains the ultimate resistance compressive force, resulting in coal fracturing and crushing, the impact energy is released, and the development of coal fractures gradually stabilize, leading to the permeability tending towards stability.

- (3) When the impact force is below the ultimate tensile load, coal permeability is more sensitive to the temperature field and corresponds to the static fracturing stage; when the impact force exceeds the ultimate tensile force but remains below the ultimate compressive load, coal permeability is more sensitive to the impact pressure field and falls into the dynamic fracturing stage.
- (4) Under low-impact loading conditions, coal permeability decreases while the slip effect occurs. When the impact load exceeds the ultimate tensile strength of coal, preexisting fractures expand outward from the interior, generating new radial (circumferential) fractures. Consequently, the slip effect diminishes and permeability increases. This mechanism provides theoretical groundwork for onsite gas drainage in

## **IAENG International Journal of Applied Mathematics**

low-permeability coal seams and borehole fracturing operations.

#### REFERENCES

- [1] J. Zhang, J. Wu, T, Yang, et al. "Analysis of fracture evolution characteristics and formation mechanism of inter-layer rock under different mining areas," Rock Mech. Rock Eng., vol. 57, no. 5, pp. 3787–3811, May 202.
- [2] G. Chen., W. Tang, S. Chen, et al. "Damage effect and deterioration mechanism of mechanical properties of fractured coal-rock combined body under water-rock interaction," Rock Mech. Rock Eng., vol. 58, no. 1, pp. 513-537, Jan. 2025.
- [3] H. Pan, H. Wang, K. Wang, et al. "Experimental study of precursory features of CO2 blasting-induced coal rock fracture based on grayscale and texture analysis," PLOS One, vol. 19, no. 2, p. e0297753, Feb. 202.
- [4] Z. Wang, H. Lian, W. Liang, et al. "Experimental study on the fracture process zones and fracture characteristics of coal and rocks in coal beds," *Rock Mech. Rock Eng.*, vol. 57, no. 2, pp. 1375–1393, Feb. 2024.
- [5] P. Wu, X. Luo, Y. Chen, et al. "Cracks propagation and permeability enhancement caused by supercritical CO<sub>2</sub> and water fracturing in natural coal-rock combination," Energy Fuels, vol. 38, no. 5, pp. 4010-4020, Mar. 2024.
- [6] Q. Qi, X. Fu, J. Kang, et al. "Study on the mechanical parameters and permeability of coal reservoirs at different temperatures," ACS Omega, p. acsomega.4c04608, Jul. 2024.
- [7] D. Zhang, H. Gao, P. G. Ranjith, et al. "Experimental and theoretical study on comparisons of some gas permeability test methods for tight rocks," Rock Mech. Rock Eng., vol. 55, no. 6, pp. 3153-3169, Jun. 2022.
- [8] Z. Lu, L. Wang, S. Wu, et al. "Investigation of pore structure and adsorption/desorption properties of coal in the non-uniform stress zone: implications for coal and gas outburst," Nat. Resour. Res, vol. 33, no. 3, pp. 1247–1268, Jun. 2024.
- [9] Y. Li, S. Zhang, and X. Zhang. "Classification and fractal characteristics of coal rock fragments under uniaxial cyclic loading conditions," Arabian J. Geosci, vol. 11, no. 9, p. 201, May 2018.
- [10] Y. Li, X. Jiang, J. Tang, et al. "Simulation study of acid fracturing initiation with consideration of rock mechanics parameter variations," *Rock Mech. Rock Eng.*, vol. 57, no. 8, pp. 5743–5761, Aug. 2024.
- [11] X. Chang, E. Xu, Y. Guo, C. Yang, Z. Hu, et al., "Experimental study of hydraulic fracture initiation and propagation in deep shale with different injection methods," J. Pet. Sci. Eng., vol. 216, p. 110834, Sep. 2022.
- [12] J. Ying, Z. Xie, Z. Jiang, et al. "Microscale fracture and creep analysis of 3D porous graphene-based cementitious material by

- nanoindentation test and energy-based method," Constr. Build. Mater., vol. 409, p. 133992, Dec. 2023.
- [13] J. Wei, A. Zhang, J. Li, et al. "Study on microscale pore structure and bedding fracture characteristics of shale oil reservoir," *Energy*, vol. 278, p. 127829, Sep. 2023.
- [14] J. T. Birk, J. Morris, J. R. Bargar, et al. "A new modeling framework for multi-scale simulation of hydraulic fracturing and production from unconventional reservoirs." Accessed: Mar. 26, 2025.
- [15] G. Zhu, Y. Zhao, T. Zhang, et al. "Micro-scale reconstruction and CFD-DEM simulation of proppant-laden flow in hydraulic fractures," Fuel, vol. 352, p. 129151, Nov. 2023.
- [16] B. Wang "Measurement and modeling of coal adsorption-perm-eability based on the fractal method," J. Nat. Gas Sci. Eng., 2021.
- [17] C. Fan, L. Yang, H. Sun, et al. "Recent advances and perspectives of CO<sub>2</sub>-enhanced coalbed methane: experimental, modeling, and technological development." Accessed: Mar. 26, 2025.
- [18] X. Wang, Y. Deng, M. Dong, M. Guan, et al, "A simplified method for evaluating shallow slope stability of slopes based on an indirectly coupled runoff and groundwater seepage model," *Hydro* geol. J., vol. 33, no. 1, pp. 309–327, Feb. 2025.
- [19] Y. Xu, Z. Wu. "Parameter identification of unsaturated seepage model of core rockfill dams using principal component analysis and multi-objective optimization," *Structures*, vol. 45, pp. 145–162, Nov. 2022.
- [20] H. Kumar, M. K. Mishra, and S. Mishra, "Sorption capacity of Indian coal and its variation with rank parameters," J. Pet. Explor-Prod. Technol., vol. 9, no. 3, pp. 2175–2184, Sep. 2019.
- [21] J. B. Walsh, "Theoretical bounds for thermal expansion, specific heat, and strain energy due to internal stress," J. Geo phys. Res, vol. 78, no. 32, pp. 7637–7646, Nov. 1973.
- [22] J. Tao, AC. Shi, HT, Li, et al, "Thermal-mechanical modelling of rock response and damage evolution during excavation in prestressed geothermal deposits," *Int. J. Rock Mech. Min. Sci.*, vol. 147, p. 104913, Nov. 2021.
- [23] Y. Wei, Y. Feng, Z. Tan, et al. "Borehole stability in naturally fractured rocks with drilling mud intrusion and associated fracture strength weakening: a coupled DFN-DEM approach," J. Rock Mech. Geotech. Eng., vol. 16, no. 5, pp. 1565–1581, May 2024.
  [24] S. Sun, G. Wei, Z. Wang, T. Jia, et al. "Fractal characteristics of the
- [24] S. Sun, G. Wei, Z. Wang, T. Jia, et al. "Fractal characteristics of the microstructure of loaded coal based on NMR and μ-CT," Energy Sources Part A, vol. 47, no. 1, pp. 4703–4720, Dec. 2025.
- [25] S. Sun, G. Wei, Z. Wang, et al. "Fractal characteristics of the microstructure of loaded coal based on NMR and μ-CT," *Energy Sources Part A*, vol. 47, no. 1, pp. 4703–4720, Dec. 2025.
- [26] S. Zhang and X. Ma, "How does In situ stress rotate within a fault zone? Insights from explicit modeling of the frictional, fractured rock mass," *J. Geophys. Res.: Solid Earth*, vol. 126, no. 11, p. e2021JB022348, 2021.